JOURNAL OF MATERIALS SCIENCE 21 (1986) 3551–3560

Topography of etched rhombohedral faces of quartz crystals: evidence for orientation effects

M. CASTAGLIOLA, C. R. TELLIER, J. L. VATERKOWSKI
Laboratoire de Chronométrie, Electronique et Piézoélectricité, Ecole Nationale Supérieure de Mécanique et des Microtechniques, Route de Gray, La Bouloie, 25030-Besancon Cedex, France

A study has been made of the rate at which the rhombohedral faces of a natural quartz crystal are etched in a concentrated ammonium bifluoride solution. The thickness of the disturbed surface layer created by an initial mechanical lapping is estimated from rate data. The etching rate as well as this thickness are found to be sensitive to natural face orientation. The changes in the surface texture of the rhombohedral faces with repeated chemical etchings are investigated. The variation in the roughness parameters with the average depth of etch shows both directional and orientation effects. The chemical attack results in the formation of stable etch figures characteristic to the orientation of the surface on which they lie and which enlarge with repeated etchings. Finally, schematic etch figures are proposed for the differently oriented rhombohedral faces.

1. Introduction

Chemical etching of quartz plates in HF or in $NH_4F \cdot HF$ solutions [1–20] can constitute a convenient procedure to develop high frequency quartz resonators [8–18]. Hence in the past few years many experiments on cuts commonly used for stable quartz crystal resonators, such as the AT-cut [8–13], the BT-cut [12–14] and the SC-cut [14–18], have been carried out. Some of these experiments [12, 13, 15, 16, 18–20] provided evidence for a formation of final dissolution figures depending on the crystal orientation in agreement with other works [3, 21–23] showing that the etch method can constitute a chemical means of determining the crystal symmetry.

In terms of the structural effect previously proposed by Ernsberger [1] to explain the variation of the dissolution rate of quartz plates with the crystal orientation, the dissolution mechanism is primarily determined by the atomic arrangement at the exposed surface of a quartz specimen. Moreover, the growth of a quartz crystal results in the development of natural rhombohedral faces intimately connected with the symmetry and the structure of this crystal. Thus a detailed study of the etching of such natural faces can perhaps permit a better understanding of the structural effect in chemical etching of quartz plates. To our knowledge there is an almost complete lack of experimental work devoted to the systematic study of the formation of etch patterns on the rhombohedral faces of quartz crystals. Hence, the purpose of this paper is to report investigations of the changes with prolonged etching in the surface topography of quartz plates whose orientations are the same as those of natural faces.

2. Experimental techniques

The plates were cut from a single natural quartz crystal. Four orientations (Ψ, θ) corresponding to the growth surfaces $(\bar{1}\,2\,\bar{1}\,1)$, $(\bar{1}\,2\,\bar{1}\,1)$, $(\bar{1}\,6\,\bar{5}\,1)$, $(\bar{1}\,0\,1\,1)$ and $(1\,0\,\bar{1}\,1)$ were selected (Table I). The orientations (Ψ, θ) (Fig. 1) were determined by using a double X-ray goniometer which offers an accuracy of about 30 sec. In this study plano-convex resonators plates were used. Before these plates were etched they were lapped with a 5 μm abrasive. The etchant was a concentrated $NH_4F \cdot HF$ solution [11] which is commonly employed in the etching of quartz. The plates were treated with this solvent at a constant temperature of 325 K.

The primary tool used at any time of etching to evaluate the changes in the surface topography was a microprocessor-based profilometer. This was supplemented at the etching times of 30, 70, 100 and 190 min with scanning electron microscopy (SEM). The scanning electron micrographs were taken with an acceleration voltage of 1 kV in order to avoid the deposition of a conducting layer on the quartz plates between successive immersions in the $NH_4F \cdot HF$ etchant.

3. Results

3.1. Rate against time of etching

The decrement, Δd, in thickness of plano-convex quartz resonator plates which oscillate in a thickness mode was evaluated from frequency measurements by

TABLE I The rhombohedral faces of a natural quartz crystal

Label	Rhombohedral face	Orientation (deg)	
		Ψ	θ
R	$\bar{1}\,0\,1\,1$	120	38.21
r	$1\,0\,\bar{1}\,1$	−60	38.21
S	$\bar{1}\,2\,\bar{1}\,1$	30	24.44
X	$\bar{1}\,6\,\bar{5}\,1$	8.94	8.048

0022–2461/86 $03.00 + .12

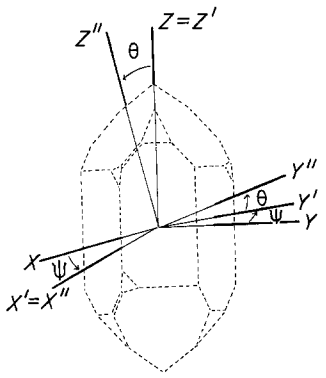

Figure 1 Singly and doubly rotated plates of quartz crystal.

means of the formula [24]

$$\Delta d = -K\frac{\Delta f}{f_i f_f} \quad (1)$$

where the constant K depends on the crystal plate orientation and on the overtone of the vibration. Δf is the change in the resonance frequency caused by chemical etching and f_i and f_f are the initial and final frequencies.

Assuming that the decrement in thickness of the quartz plates varies linearly with the time, t, of etching, as previously observed [11, 15, 18] for differently oriented quartz resonator plates, average values of the dissolution rate R were evaluated for successive intervals of the etching time. The results for the four samples are shown in Fig. 2. All the curves are characterized in the initial stages of etching by a relatively rapid decrease in the dissolution rate which tends to a limiting value depending on the crystal orientation.

3.2. Surface profilometry

Two rectangular traces were made to investigate the changes in surface profiles and in roughness parameters with the average depth, $\Delta d_S = \Delta d/2$, of etch of a resonator surface. If possible one of these traces, denoted for convenience $\alpha_{\Psi,\theta}$, coincides with a particular crystallographic direction (Table II). Taking into account the digonal symmetry of the crystallographic X-axis, only modifications in the plane surface of r and R quartz resonators were given. Average values of two widely used [25] roughness parameters, the centre line average roughness, R_a, and the root mean square (r.m.s.) roughness, R_q, were evaluated from these two traces.

TABLE II The two profilometry traces for the differently oriented faces

Rhombohedral face	$\alpha_{\Psi,\theta}$ trace	$\beta_{\Psi,\theta}$ trace
R	Crystallographic X axis	Z'' direction
r	Crystallographic X axis	Z'' direction
S	Crystallographic Y axis	Z'' direction
X	X' direction	Z'' direction

There are three particularly interesting features of the variations in roughness parameters with the depth of etch as revealed by Figs 3 and 4.

1. The shape of R_a and R_q against Δd_S plots depends, for a given orientation, on the direction of measurement. The behaviour of X or r plates particularly bears evidence of this directional effect. Effectively turning to the plane surface of the X plate, repeated etchings cause a moderate increase and a marked decrease in roughness parameters measured along the respective $\alpha_{\Psi,\theta}$ and $\beta_{\Psi,\theta}$ directions.

2. For given α and β traces, the roughness parameter–depth of etch behaviour is found to be orientation dependent. For example, data obtained on roughness parameters for stylus traces made along the $\beta_{\Psi,\theta}$ direction of the plane surface of r and X plates reveal a marked decrease for the X plate and an increase followed by a further decrease for the r plate. Even for traces made along the crystallographic X-direction, which is common to r and R plates, successive etchings produce a decrease in roughness parameters which occurs more rapidly for r plates than for R plates.

3. In the case of doubly rotated S and X plates, we observe differences in the changes of roughness parameters on etching calculated from traces made on the two surfaces of these plates. This effect is conveniently illustrated by roughness data obtained for the $\alpha_{\Psi,\theta}$ direction of the two X surfaces (curves a and b, Fig. 3).

Surface profiles displayed in Figs 5 to 10 agree well with these features. Figs 5a and 6a give evidence for orientation effects, whereas marked directional effects

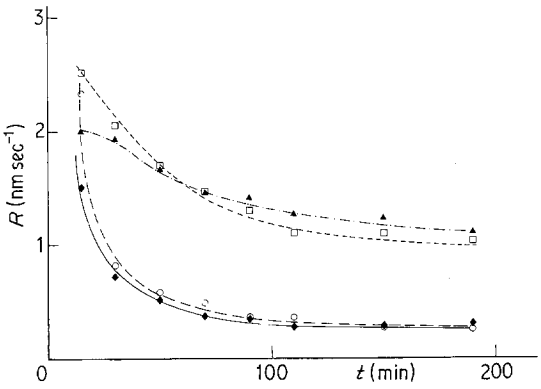

Figure 2 The dissolution rate, R, as a function of the depth, Δd_S, of etch of differently oriented quartz plates. ○, r; □, R; ▲, S; ◆, X.

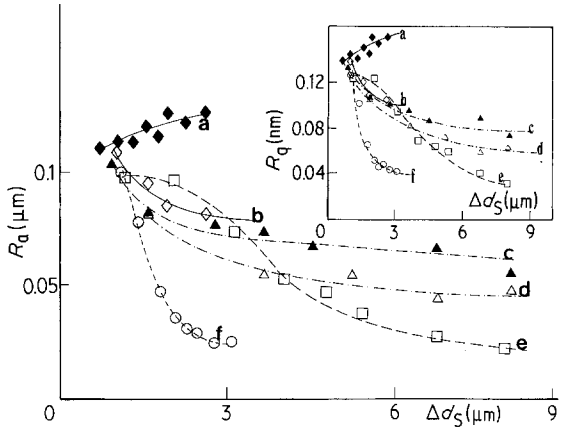

Figure 3 The roughness parameter, R_a, as measured along the $\alpha_{\Psi,\theta}$ direction of the various rhombohedral faces against the depth, Δd_S, of etch. In the inset are shown the R_q against Δd_S plots. ◆, X plane; ◇, X convex; ○, r; □, R; ▲, S plane; △, S convex.

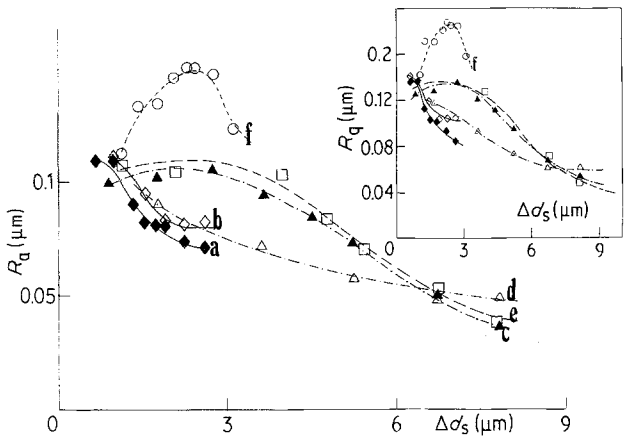

Figure 4 The roughness parameter, R_q, as measured along the $\beta_{\Psi,\theta}$ direction of the various rhombohedral faces against the depth, Δd_S, of etch. In the inset are shown the R_q against Δd_S plots. ◇, X plane; ◇, X convex; ○, r; □, R; ▲, S plane; △, S convex.

are revealed by Fig. 5 or 7. The revelant surface profiles along the α and β traces of the two surfaces of X and S plates shown in Figs 7 to 10 also indicate differences in the final surface shape developed on the two surfaces of these doubly rotated cuts.

3.3. Scanning electron micrographs

Scanning electron micrographs of the differently oriented plates are presented in Figs 11 to 16 at various stages of etching. Whatever the orientation, prolonged etching causes an enlargement of the etch patterns. But this is the only behaviour which remains unaffected by the crystal orientation. Successive etchings in an $NH_4F \cdot HF$ solution produce etch figures which are unlike in form those for the different natural faces. Well-defined etch figures, all uniformly oriented and shaped, are obtained upon the r plate after repeated immersions in $NH_4F \cdot HF$. The figures consist of triangular depressions with a curved side elongated markedly along the X-axis (Fig. 11). In general, the final etch figures formed on the R plate are flat-bottomed depressions with five or six curved sides extending slightly in the direction of the X-axis (Fig. 12). The figures upon the plane surfaces of X plates differ more and less in the initial and final stages of etchings (Fig. 13). The final etch figures are irregular pits with rather undefined curved faces uniformly elongated parallel to the $\beta_{\Psi,\theta}$ direction.

The results obtained on the convex surface are quite different. The figures, which are terraced depressions and extend in a direction γ_X lying about 130° anticlockwise with respect to the X' axis, may be identified as triangular grooves with curved sides (Fig. 14). Prolonged etching of the plane surface of the S plate causes the development of terraced etch figures (Fig. 15) elongated markedly in a direction, γ_S, about 126° to the crystallographic Y-axis. Etch pits composed of three or four well-defined faces and extending parallel to the γ_S direction are also present on the plane surface. All figures examined on the convex surface of S plates have a little relief, but they extend without ambiguity in the same direction. However, the figures produced on the convex surface are essentially different from those formed upon the other face: they seem to be composed of convex terraces with a curved side less extended than the terraced figures produced on the plane surface (Fig. 16).

TABLE III The critical depth of etch at which the rate is determined by the face orientation

Rhombohedral face	Estimated thickness of the disturbed surface layer (μm)
R	5
r	2.4
S	5
X	1.9

4. Discussion

First, some remarks can be made on the dissolution rate data. Some authors [8, 11, 12, 15, 26, 27] suggested that the initial surface damage can markedly influence the dissolution rate. Figs 3 and 4 indicate effectively that in the initial stage of etching the differently oriented quartz plates exhibit approximately the same average geometrical surface properties as expected for quartz plates which have suffered the same mechanical preparation process. But this similarity tends to disappear as the crystals etch. From the curves of Fig. 2 it appears that the rate becomes a characteristic of the crystal orientation. The depth of etch at which the rate is determined principally by the orientation was estimated (Table III) from these curves for the various faces. As this depth of etch is usually [27] identified with the thickness of the disturbed layer created by the initial mechanical lapping [10, 27–29] the results displayed in Table III suggest that the disturbed surface layer is not only a function of the abrasive particle size

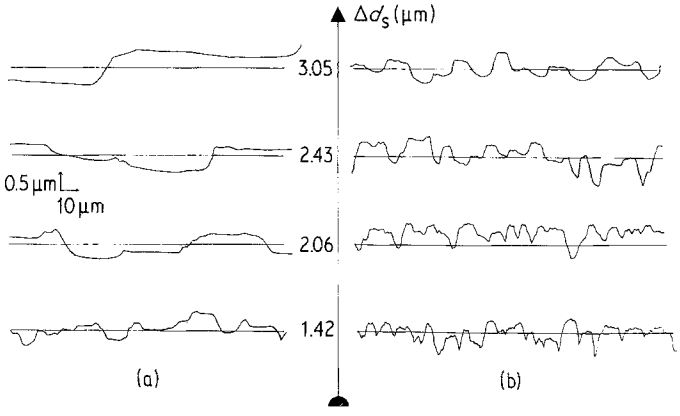

Figure 5 Changes in the profilometry traces made (a) along the X direction and (b) along the $\beta_{\Psi,\theta}$ direction of an r face.

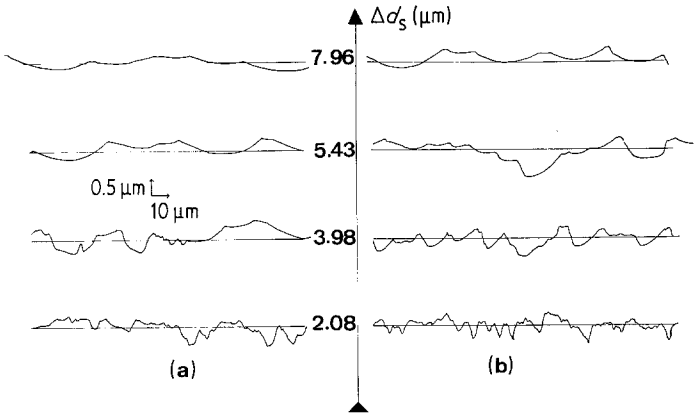

Figure 6 Changes in the profilometry traces made (a) along the *X*-direction and (b) along the $\beta_{\Psi,\theta}$ of an R face.

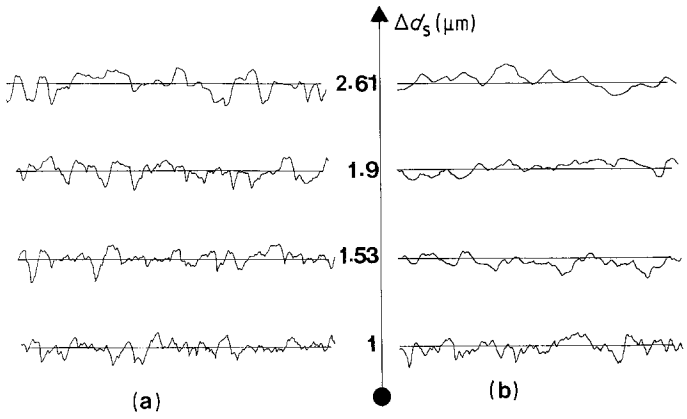

Figure 7 Changes in the profilometry traces made (a) along the $\alpha_{\Psi,\theta}$ direction and (b) along the $\beta_{\Psi,\theta}$ direction of the plane surface of an X face.

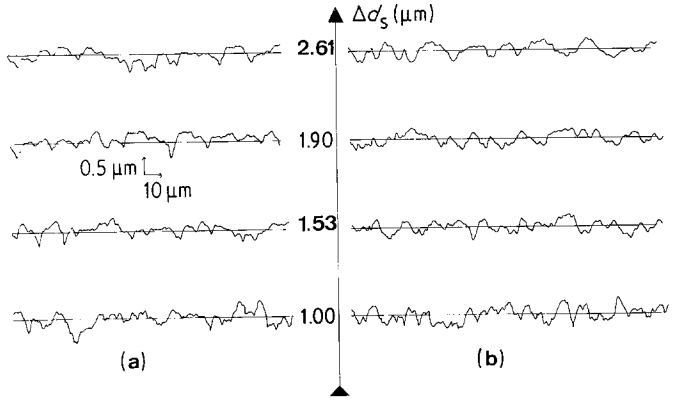

Figure 8 Changes in the profilometry traces made (a) along the $\alpha_{\Psi,\theta}$ direction and (b) along the $\beta_{\Psi,\theta}$ direction of the convex side of an X face.

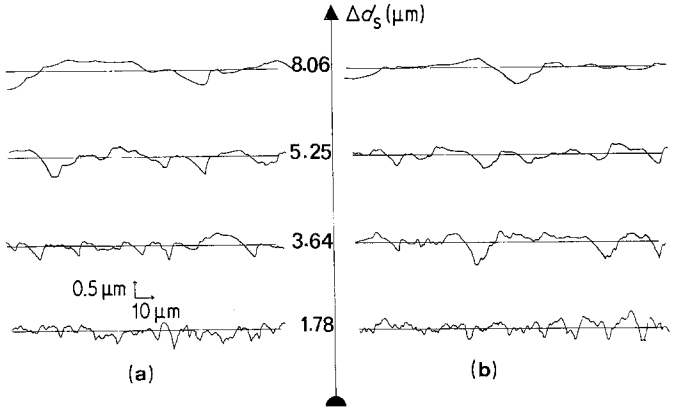

Figure 9 Changes in the profilometry traces made (a) along the *Y* direction and (b) along the $\beta_{\Psi,\theta}$ direction of the plane surface of an S face.

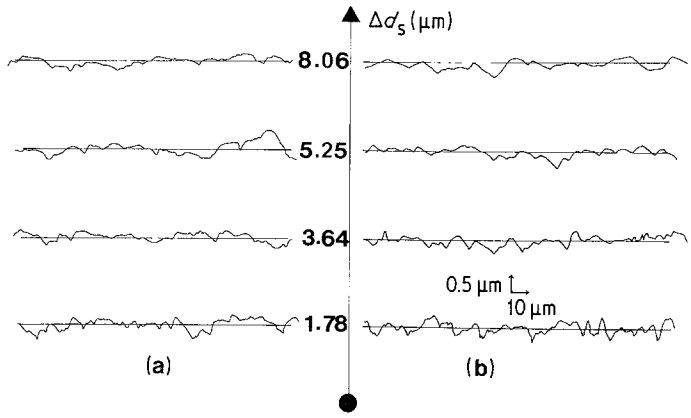

Figure 10 Changes in the profilometry traces made (a) along the Y direction and (b) along the $\beta_{\Psi,\theta}$ direction of the convex side of an S face.

but is also sensitive to the crystal orientation. This observation agrees with previous results upon single crystal germanium [27].

It is also possible to compare these rate data with previous works [11–13, 16, 20] on singly and doubly rotated cuts in which kinetics studies of the dissolution process were undertaken. Assuming that the dissolution rate can be described in terms of an Arrhenius equation [2, 11–13, 15, 30]

$$R = A \exp\left(-\frac{E_a}{k_B T}\right) \quad (2)$$

where k_B is the Boltzmann constant and T the absolute temperature, and taking an average value of about 0.4 eV [11–13, 15, 16, 18–20, 31] for the apparent activation energy, E_a, the final dissolution rates were evaluated at a reciprocal temperature of $2.7 \times 10^{-3} K^{-1}$ (Table IV). In Table IV the rate data, obtained on various quartz plates whose orientations do not depart very much from those of natural faces, are also given. We observe a good agreement between rate values of firstly the r faces and the BT-39 plates and secondly the X face and the Y-cut plates. We observe a discrepancy between values related to respective R face and AT-37 plates but previous kinetics studies on AT plates cut from quartz crystals with different growth histories have also revealed departures in dissolution rates which varied in the range 3 to 8 nm sec^{-1}. Thus as expected the value of 5.8 nm sec^{-1} obtained for the R face remains in the same range.

We can also comment on the various etch patterns formed on the differently oriented faces. On the one hand it might be of interest to compare these patterns firstly with those produced on Y [3, 13, 16, 19], AT-37 [20] and BT-49 [15] plates, and secondly with dissolution figures presented in literature [3, 6, 7] and concerned with natural faces. Typical variations in roughness parameters of the AT-37 plate [20] produced by successive etchings resulted in curves similar to curves related to the R face. Comparison of the dissolution figures formed on the AT-37 plate and R face shows that the dissolution process plays an identical role in the development of etch patterns which is essentially governed by the crystal orientation. The R_a against d_S plot of respective r face and BT-49 cut [15] exhibits nearly the same behaviour depending strongly on the direction of measure. The fact that the etch figures produced on both r and BT-49 plates are markedly elongated along the crystallographic X direction can certainly account for the similarity in the experimental curves. Effectively, when the depth of etch does not exceed 4 μm for the two plates, the difference between the etch patterns formed on r and BT-49 plates [15] is not great and the elongation of the dissolution figures along the X axis remains the dominant feature of the chemical attack. Successive etchings on the plane or convex side of the X plate reveal (Figs 13 and 14) some particular pits which appear as triangular depressions with a curved side slightly elongated in the Z'' direction (Fig. 1). It must be pointed out that these pits present a similarity with the etch figures which develop on Y-cut quartz plates and which consist of triangular depressions extending along the Z direction [3, 13, 16, 19].

It is reasonable to asume that the mechanical lapping produces pits which can sometimes expose natural faces and that, in general, the etch figures of mechanical pits are mainly determined by the inclination of these pits to the rhombohedral X face. In these conditions, a chemical attack on a mechanically pitted X face can reveal particular etch figures exhibiting a stable shape during repeated etchings and corresponding to a surface whose orientation is not far from that of this X face. As for a natural X face, the angle θ and Ψ take values less than 10° when these two conditions are met by a Y-cut surface. But as an optically flat Y-cut plate etches slower than a natural X face [13] the density of these typical etch pits generated by a mechanical lapping will be lowered by successive etchings. Examination of Figs 13 and 14 shows a satisfactory agreement with this description.

TABLE IV Etching rate (at $T^{-1} = 2.7 \times 10^{-3} K^{-1}$) for various orientations

Crystal surface		Etching rate (nm sec^{-1})
R		5.8
r		1.4
S		6.3
X		1.7
AT-37* ($\Psi = 0, \theta = 37.5°$)	AT-37-1	3.6
	AT-37-2	3
BT-39 ($\Psi = 0, \theta = -39°$)	BT-39-1	1.7
	BT-39-2	1.4
Y-cut† ($\Psi = 0, \theta = 0$)	Y-2	1.2
	Y-3	0.8

*Data from [20].
†Data from [13, 16].

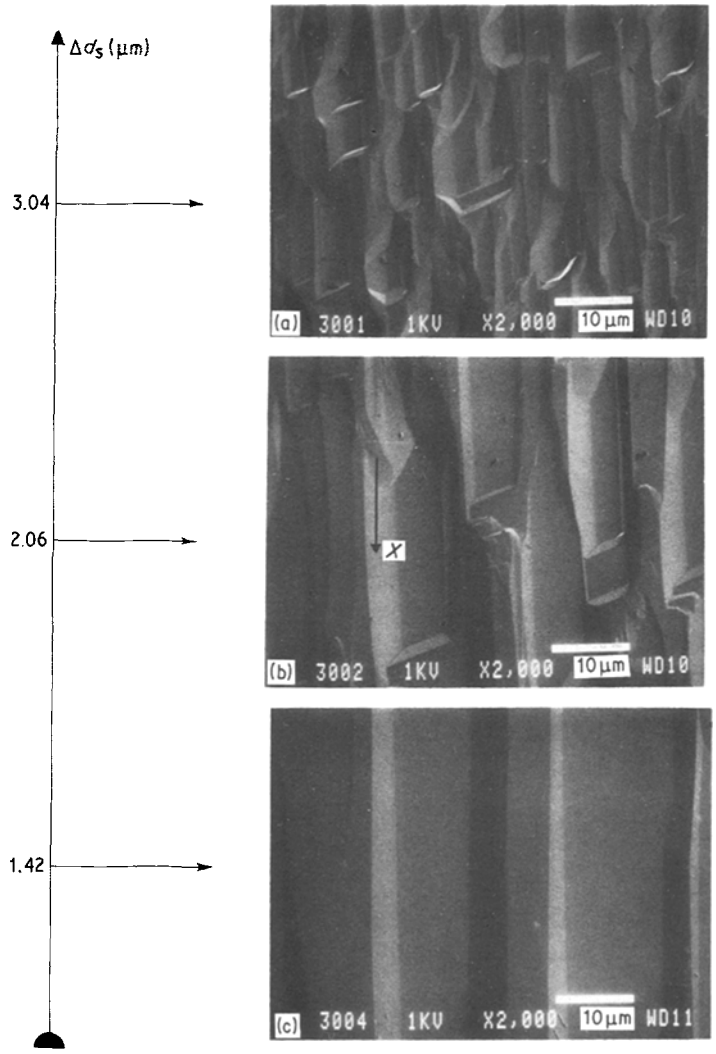

Figure 11 Scanning electron micrographs for the r face: (a) $\Delta d_S = 1.42\,\mu m$, (b) $\Delta d_S = 2.06\,\mu m$, (c) $\Delta d_S = 3.05\,\mu m$.

A comparison of previously published works [3–7, 21] with the present study can be undertaken but this comparison can be regarded as fragmentary because most of these works were concerned with unusual etch pits [4, 21] or with an evaluation of the structural perfection of both synthetic or natural quartz crystals [5–7, 21] and were carried out on r and R faces only [3, 5–7]. The study of etch patterns on the r and R faces of synthetic quartz crystals by Augustine and Hall [6] gave relatively poorly defined pits, except etch pits running deep into the observed faces which can be considered as unusual pits. The etched R surface appeared as undulated but the r face was covered with numerous triangular pits. These features present some similarity with the etch patterns shown in Figs 11 and 12. Patel *et al.* [7] reported some investigation on the etch patterns produced by hydrogen fluoride on cleaved $(1\,0\,\bar{1}\,1)$ rhombohedral faces. The shape of the etch pits, faintly visible, roughly resembled elongated triangles but unfortunately the direction of elongation of these pits was not identified. Only Wegner and Christie [3] carefully described the etch pits revealed on the r face of a quartz crystal etched with ammonium bifluoride and reported that triangles with pointed bottoms, slightly extended along the *X*-axis, resulted from immersion in saturated $NH_4F \cdot HF$ for 5 h. For a saturated ammonium bifluoride etchant maintained at room temperature, we can estimate that after 5 h the depth of etch of an r face reaches a value of about 1 μm, and the shape of etch pits reported by Wegner and Christie corresponds to our etch patterns presented in Fig. 11a. Even if the comparison with results reported in the literature cannot be complete because of a particular lack of informations on S and X faces, we may note that our study is in agreement with previous results on r and R faces and has the advantage of giving much more detail on the surface topography of etched rhombohedral faces. The main feature is that chemical etching gives rise to a topography associated with the crystal orientation. It should be emphasized that the comparison gives some evidence of an absence of influence of the initial surface damage on the final texture of deeply etched quartz faces.

To establish without ambiguity that the final shape of etch pits and the initial surface damage are unconnected, we have also performed a chemical etching at 294 K for 15 h on a natural R face which was free of initial mechanical treatment. As this chemical attack on such an R face yields etch pits whose shape, size and density are quite similar to those observed on initially lapped R faces etched to about 6 μm, we can conclude that the crystal orientation is the factor governing the final topography of natural quartz faces immersed in a concentrated ammonium bifluoride etchant. As the shape of etch pits, which is intimately connected with the crystal orientation, is a characteristic of the crystal symmetry it might be of interest to propose a schematic drawing (Fig. 17) of the etch

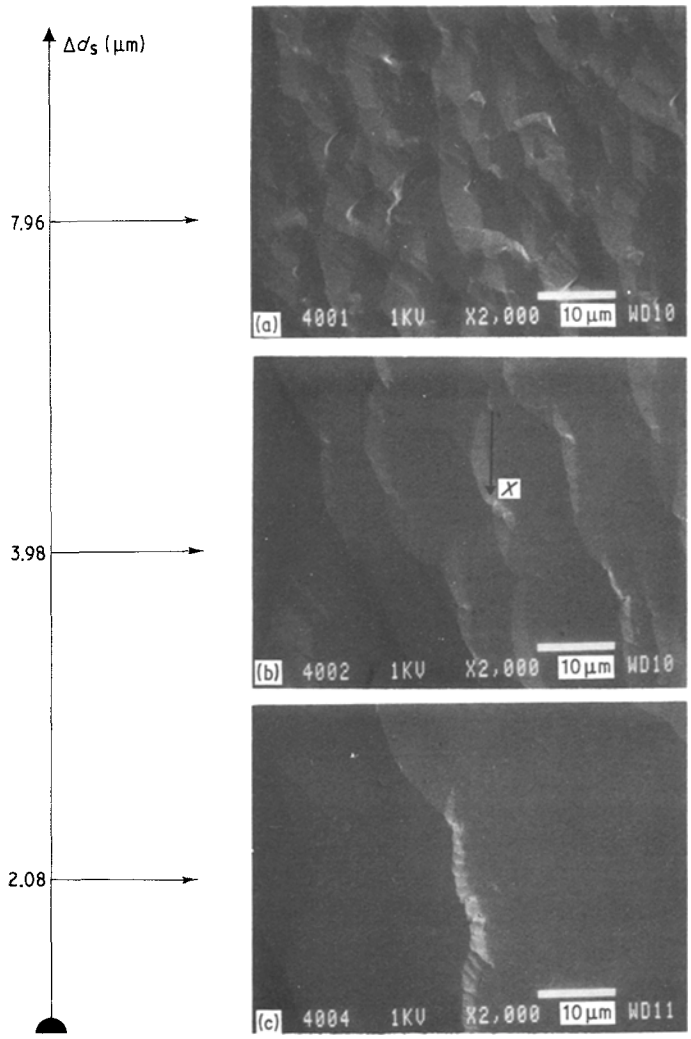

Figure 12 Scanning electron micrographs for the R face: (a) $\Delta d_S = 2.08\,\mu m$, (b) $\Delta d_S = 3.98\,\mu m$, (c) $\Delta d_S = 7.96\,\mu m$.

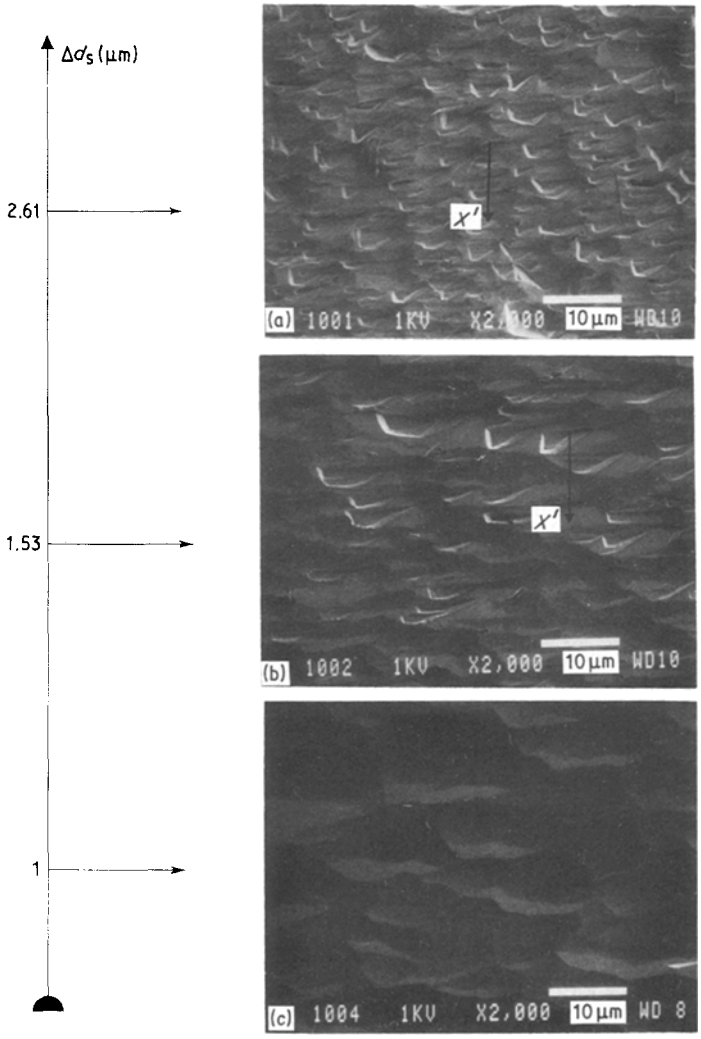

Figure 13 Scanning electron micrographs for the plane surface of the X face: (a) $\Delta d_S = 1\,\mu m$, (b) $\Delta d_S = 1.53\,\mu m$, and (c) $\Delta d_S = 2.61\,\mu m$.

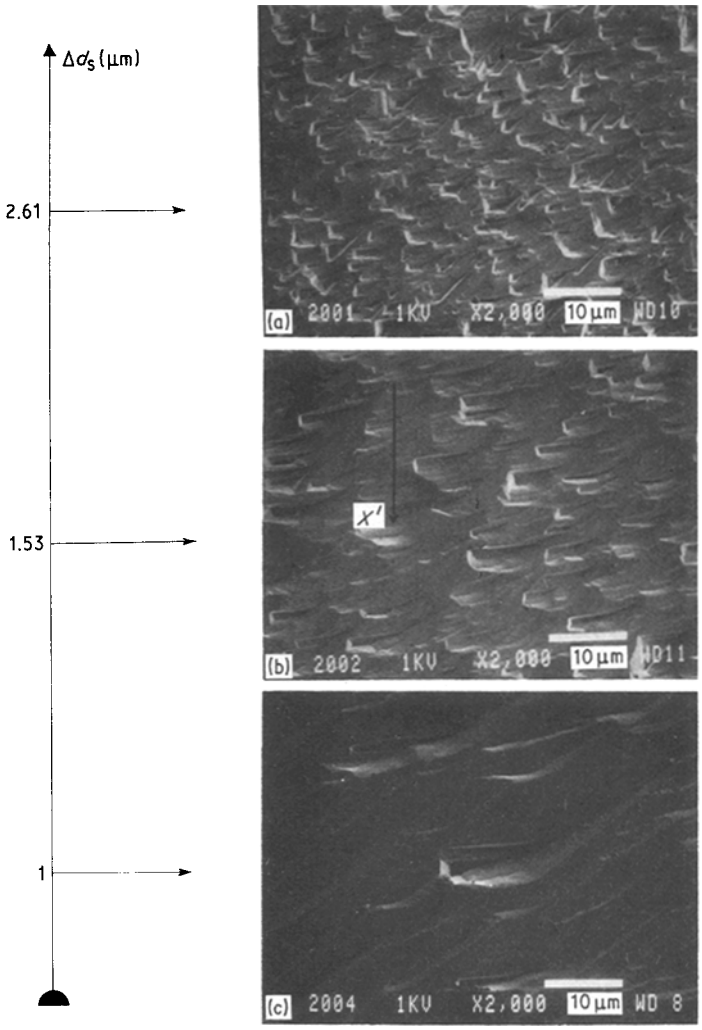

Figure 14 Scanning electron micrographs of the convex surface of the X face: (a) $\Delta d_S = 1\,\mu m$, (b) $\Delta d_S = 1.53\,\mu m$, (c) $\Delta d_S = 2.61\,\mu m$.

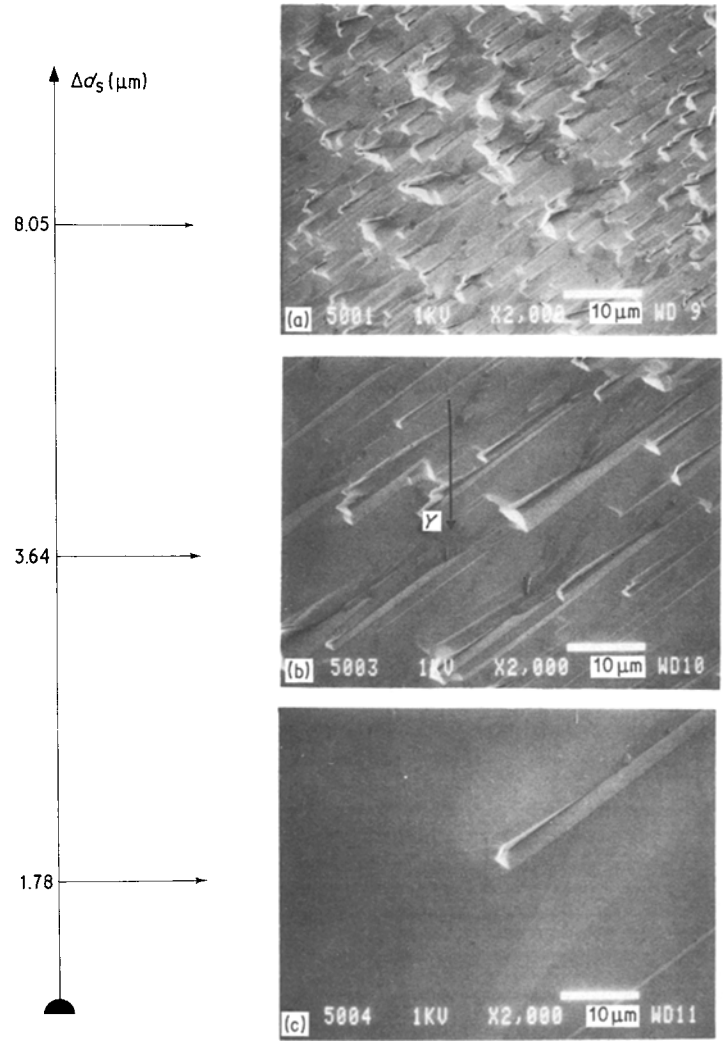

Figure 15 Scanning electron micrographs of the plane surface of the S face: (a) $\Delta d_S = 1.78\,\mu m$, (b) $\Delta d_S = 3.64\,\mu m$, (c)$\Delta d_S = 8.05\,\mu m$.

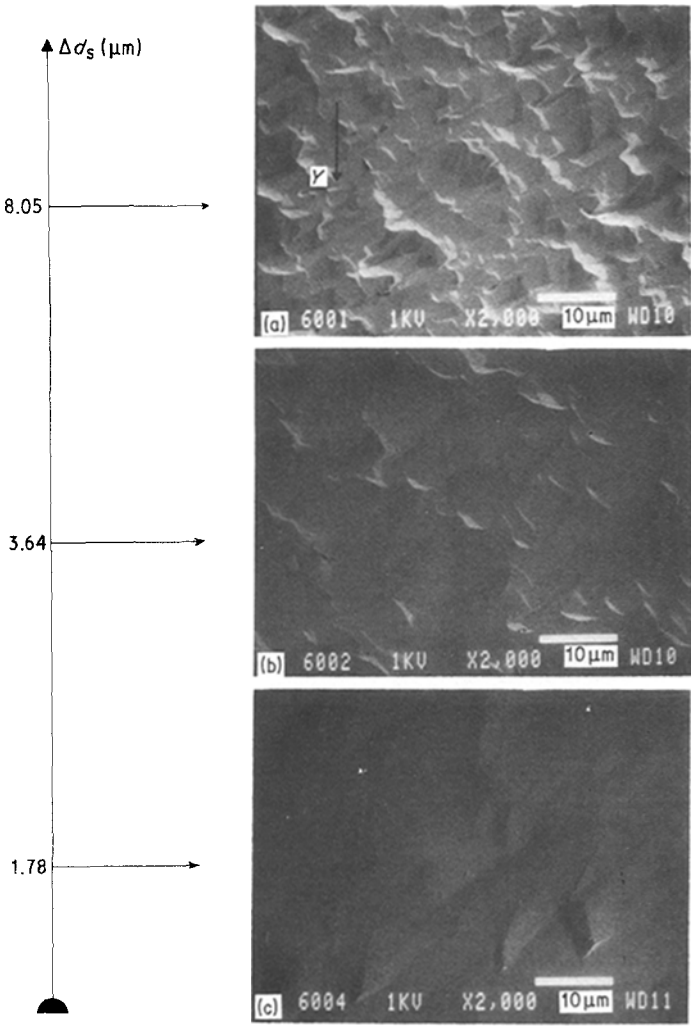

Figure 16 Scanning electron micrographs of the convex surface of the S face: (a) $\Delta d_S = 1.78\,\mu m$, (b) $\Delta d_S = 3.64\,\mu m$, (c) $\Delta d_S = 8.05\,\mu m$.

figures which develop on the rhombohedral faces of quartz crystal, since no drawing has been presented to date.

5. Conclusions

The etching rate of the various rhombohedral faces is found to be strongly dependent on face orientation. From the variation of the rate with the etching time the thickness of the disturbed layer due to initial mechanical lapping is estimated. It appears that this thickness also varies with orientation.

The study of the changes in roughness parameters and in etch patterns with successive etchings leads to the following conclusions:

1. In agreement with the 32 point symmetry group of quartz crystal, the etch patterns for the r and R faces which develop on the two sides are similar. For the same reason, etching produces etch figures of different shape on the two sides of X and S plates.
2. The variation of the roughness parameters with the average depth of etch reveals directional effects and a marked sensitivity to the surface orientation.
3. The final shape of the etch figures is uniquely determined by the orientation of the rhombohedral face, since the initial surface damage has no influence on the final etch pattern as shown by results on lapped and initially free of damage R plates.

From these conclusions, which all together bear evidence for an etching process governed by the crystal orientation, it is possible to reply to lack of information on the etching of rhombohedral faces of quartz crystal by proposing a schematic drawing of the etch figures produced by a prolonged immersion of these natural faces in a concentrated ammonium bifluoride solution.

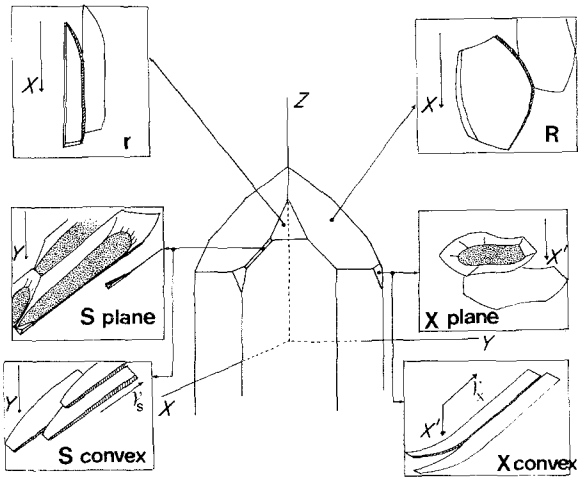

Figure 17 Schematic etch figures for the rhombohedral faces of a natural quartz crystal.

References

1. F. M. ERNSBERGER, *J. Phys. Chem. Solids* **113** (1960) 347.
2. V. V. SOROKA, E. I. LAZORINA and V. N. STEPANCHUK, *Sov. Phys. Crystallogr.* **22** (1977) 353.
3. M. W. WEGNER and J. M. CHRISTIE, *Phys. Chem. Minerals* **9** (1983) 67.

4. J. W. NIELSEN and F. G. FOSTER, *Amer. Mineral.* **45** (1960) 299.
5. A. R. LANG and V. F. MIUSCOV, *J. Phys.* **38** (1967) 2477.
6. F. AUGUSTINE and D. R. HALE, *J. Phys. Chem. Solids* **13** (1960) 344.
7. A. R. PATEL, O. P. BAHL and A. S. VAGH, *Acta Crystallogr.* **19** (1965) 757.
8. J. R. VIG, J. W. LEBUS and R. FILLER, Report no. ECOM-4548 (US Army Electronic Research and Development Command, Fort Monmouth, New Jersey, 1977).
9. D. ANG, in Proceedings of the 32nd Annual Symposium on Frequency Control, Fort Monmouth, New Jersey, 1978 (Electronic Industries Association, Washington, DC, 1978) p. 282.
10. H. FUKUYO and N. OURA, in Proceedings of the 30th Annual Symposium on Frequency Control, Fort Monmouth, New Jersey, 1976 (Electronic Industries Association, Washington, DC, 1976) p. 254.
11. C. R. TELLIER, *J. Mater. Sci.* **17** (1982) 1348.
12. *Idem, Surf. Technol.* **21** (1984) 83.
13. *Idem,* in Proceedings of the 38th Annual Symposium on Frequency Control, Philadelphia, Pennysylvania, 1984 (Institute of Electronic and Electrical Engineers, New York, NY, 1984) p. 105.
14. J. R. VIG, R. J. BRANDMAYR and R. L. FILLER, Report no. DELET-TR-80-5 (US Army Electronics Research and Development Command, Fort Monmouth, New Jersey, 1980).
15. C. R. TELLIER and C. B. BURON, *Surf. Technol.* **22** (1984) 287.
16. C. R. TELLIER, in Proceedings of the XIth International Congress of Chronometry, Besançon, France, 1984 (Société Française des Microtechniques et de Chronométrie, Besançon, France, 1984) p. 115.
17. R. J. BRANDMAYR and J. R VIG, Report no. DELET-TR-81-16 (US Army Electronics Research and Development Command, Fort Monmouth, New Jersey, 1981).
18. C. R. TELLIER, C. BURON and F. JOUFFROY, *Mater. Chem. Phys.* **14** (1986) 25.
19. C. R. TELLIER and F. JOUFFROY, *J. Mater. Sci.* **18** (1983) 3621.
20. C. R. TELLIER, in Proceedings of the 39th Annual Symposium on Frequency Control, Philadelphia, Pa, May 1985 (Institute of Electronic and Electrical Engineers, New York, 1985) p. 282.
21. R. B. HEIMANN, in "Silicon Chemical Etching", edited by J. Grabmaier (Springer, Berlin, 1982) pp. 197–207.
22. A. P. HONESS, "The Nature, Origin and Interpretation of the Etch Figures on Crystals" (Wiley, New York, 1927) Chs III and VI.
23. K. H. YANG, *J. Electrochem. Soc.* **131** (1984) 1140.
24. C. LU, in "Applications of Piezoelectric Quartz Crystal Microbalances" edited by C. Lu and A. W. Czanderna (Elsevier, Amsterdam, 1984) Ch. 2.
25. T. R. THOMAS, "Rough Surfaces" (Longman, London, 1981) Ch. 4.
26. B. A. IRVING, in "The Electrochemistry of Semiconductors", edited by P. J. Holmes (Academic Press, London, 1962) pp. 256-89.
27. P. R. CAMP, *J. Electrochem. Soc.* **102** (1955) 586.
28. J. VIG, H. WASSHAUSEN, C. COOK, M. KATZ and E. HAFNER, in Proceedings of the 27th Annual Symposium on Frequency Control, Fort Monmouth, New Jersey, 1974 (Electronic Industries Association, Washington, DC, 1974) p. 98.
29. Y. SEKIGUCHI and H. FUNAKUBO, *J. Mater. Sci.* **15** (1980) 3066.
30. H. EYRING and E. M. EYRING, "Modern Chemical Kinetics" (Reinhold, New York, 1965).
31. J. S. JUDGE, *J. Electrochem. Soc.* **118** (1971) 1772.

Received 28 October
and accepted 20 December 1985